in series following the designations given by Garton and Codling.[9] Unless otherwise stated the wavelengths are those reported by Garton and Codling. No attempt has been made to analyze these lines in terms of Fano resonance profiles as this has recently been done between 2024 and 1722 Å by Garton, Grasdalen, Parkinson, and Reeves,[10] and below 1722 Å the lines are essentially symmetrical. Table VIII presents the wavelengths and oscillator strengths of unidentified and miscellaneous lines observed.

ACKNOWLEDGMENTS

We sincerely thank Dr. R. A. Becker for his help and encouragement in this work and M. E. Brennan and R. Marcoe for their able technical assistance.

*Presently at the University of Salford, Salford, England.

[1]W. R. S. Garton, A. Pery, and K. Codling, in Proceedings of the Fourth International Conference on Ionization Phenomena in Gases, Uppsala, 1959 (North-Holland Publishing Co., Amsterdam, 1960), p. 206.

[2]R. D. Hudson, V. L. Carter, and J. A. Stein, J. Geophys. Research 71, 2295 (1966).

[3]R. D. Hudson, Phys. Rev. 135, 1212 (1964).

[4]R. D. Hudson and V. L. Carter, Phys. Rev. 137, 1648 (1965).

[5]R. Hultgren, R. L. Orr, P. D. Anderson, and K. K. Kelley, in Selected Values of Thermodynamic Properties of Metals and Alloys (John Wiley & Sons, Inc., New York, 1963).

[6]R. E. Honig, RCA Rev. 23, 567 (1962).

[7]A. N. Nesmeyanov, in Vapor Pressure of the Chemical Elements, edited by Robert Gary (Elsevier Publishing Co., New York, 1963).

[8]R. D. Hudson and V. L. Carter, J. Opt. Soc. Am. 58, 227 (1968).

[9]W. R. S. Garton and K. Codling, J. Phys. B, 1, 106 (1968).

[10]W. R. S. Garton, G. L. Grasdalen, W. H. Parkinson, and E. M. Reeves, J. Phys. B, 1, 114 (1968).

PHYSICAL REVIEW VOLUME 180, NUMBER 1 5 APRIL 1969

Optical Pumping of Neon $^3P_2$ Metastable Atoms

L. D. Schearer

Texas Instruments Incorporated, Dallas, Texas

(Received 23 December 1968)

The $^3P_2$ metastable atoms of neon have been optically oriented. This represents the first case of the optical pumping of non-S state atoms. The optical-pumping process is described, and depolarization cross sections for collisions with ground-state neon and ground-state helium atoms measured. The cross section for collisional depolarization with helium is 4.30 $\pm$ 0.22 $\times 10^{-17}$ cm^2, and with neon is 166 $\pm$ 8 $\times 10^{-17}$ cm^2 at 300° K. The metastable $^3P_2$ atoms of Ar and Xe have also been optically pumped. As the polarizability of the noble-gas buffer increases, the collisional depolarization cross section approaches the diffusion cross section.

I. INTRODUCTION

The conventional method of optical pumping introduced by Dehmelt[1] has been applied successfully in the past only to those atoms possessing a ground electronic state of zero angular momentum ($L = 0$). In particular, the optical orientation and detection of atoms has been confined to the alkali atoms ($^2S_{1/2}$),[2,3] Hg($^1S_0$),[4] and He($^3S_1$).[5,6] Engineering difficulties have precluded the optical orientation of other S-state atoms[7] with nonzero spin, while for atoms possessing orbital angular momentum ($L > 0$), it has generally been assumed that considerable depo-

larization would result from collisions with a nonmagnetic buffer gas or the container walls. Atoms having a non-S configuration would then have a very fast spin relaxation time, and the accumulation of an observable spin polarization would be impossible.[8]

Depolarization cross sections on the order of 10^{-14} cm^2 for atoms with a P configuration colliding with noble-gas atoms have been measured for a variety of atoms which tends to support the preceding hypothesis.[9]

The P character of all the atoms for which depolarization cross sections are available is associated with the outer electron which is in a p orbital. Thus, it is not surprising that the observed cross sections are all on the order of the gas-kinetic cross section. These large cross sections for collisional depolarization can be compared to the remarkably small depolarization cross sections for the ground-state alkali atoms ($^2S_{1/2}$) in a buffer of noble-gas ($^1S_0$) atoms which range from 10^{-22} to 10^{-26} cm^2.[10,11]

The electron configuration for the $^3P_2$ metastable states of the noble gases Ne, Ar, Kr, and Xe is notably different from the above mentioned atoms. For example, the $^3P_2$ neon metastable atom has an electron configuration $2p^5 3s$. Here the outer electron is in an s orbital, and the orbital angular momentum is associated with the core electrons. As a matter of fact the gross structure of the noble-gas metastable atoms is similar to that of the adjacent alkali ground-state atom.[12] Both are characterized by a single s electron of principal quantum number n, plus a singly ionized p core of principal quantum number $n-1$. In the case of the alkali atoms, however, the core electrons form a closed $^1S_0$ shell, while the core electrons for the heavy noble-gas metastable atoms have a $^2P_{3/2}$ configuration.

Given this similarity between the electron configurations of the neon metastable atom and the ground-state of the sodium atom, we might reasonably expect that the collisional depolarization cross section for $^3P_2$ neon atoms would be considerably smaller than those previously measured for P states. This reduction in the magnitude of the depolarization cross section for metastable neon is thus a measure of the extent to which the $3s$ orbital electron is effective in shielding the core electrons from the perturbation resulting from a collision.

If the depolarization cross section for $^3P_2$ neon atoms in a buffer of helium gas is sufficiently small, the technique of optical pumping can yield useful polarizations and, consequently, large optical signals at resonance. In the following sections we describe the optical-pumping process in a neon-He discharge, and the measurement of the depolarization cross section for neon ($^3P_2$) metastable atoms colliding with ground-state helium and ground-state neon atoms. A preliminary account of the optical-pumping process was presented earlier.[13]

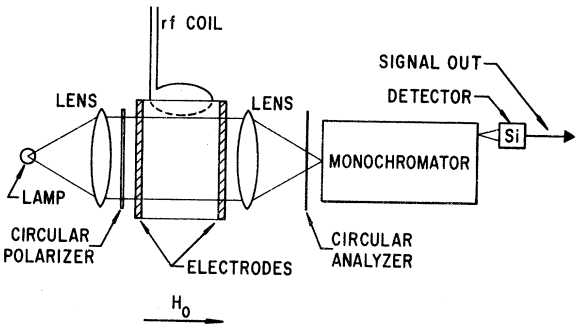

FIG. 1. Schematic diagram of apparatus.

II. EXPERIMENTAL APPARATUS AND ARRANGEMENT

The apparatus utilized in this experiment is similar to that described in earlier work in optical pumping in helium. The primary components are the neon optical-pumping lamp and the pyrex absorption cell containing a mixture of helium and neon gas. A weak rf electric field excites a discharge in the cell and maintains a small fraction of the neon atoms in the $^3P_2$ metastable level. The resonance radiation from the lamp is circularly polarized and passed through the absorption cell colinear with an external applied magnetic field. The transmitted light is focused on the slits of a grating monochromator and detected with a photovoltaic silicon cell. The experimental arrangement is shown in Fig. 1.

The lamp was filled with reagent grade neon to a pressure of about 1 Torr. Lamps containing 10% helium were also occasionally used. The lamps containing pure neon were susceptible to plasma oscillation when excited too hard. Addition of helium tended to reduce the oscillations and restore stability. The lamps were excited with 5–10 W of rf power at 50 MHz. The power was capacitively coupled to the gas using external electrodes. The resonance radiation from the lamp consists of eight lines between 5882 and 7032 Å; the most intense line at 6402 Å results from the $^3D_3$–$^3P_2$ transition. No attempt was made to filter the radiation prior to the absorption cell.

The absorption cell consisted of a Pyrex cylinder with a diffusion length $\Lambda = 1$ cm. The cells were evacuated after bakeout to 10^{-7} Torr, and reagent grade neon admitted at pressures between 2 and 40 μ Hg. The neon pressures were monitored with a Pirani gauge and a CVC Autovac reader. Absolute pressure measurements were made with a McLeod gauge. After filling with neon, helium was admitted at pressures be-

0.1 and 2 mm Hg. The total pressure was then measured with the McLeod gauge. Fifteen minutes elapsed prior to the final total-pressure measurement to insure an equilibrium mixture of the two gases.

The resonance rf magnetic field between 2 and 7 MHz was obtained from a General Radio unit oscillator which was connected to a small set of Helmholtz coils whose coil axis was orthogonal to the external dc magnetic field. The coil current was square-wave modulated at 400 Hz by interrupting the oscillator cathode current. A variable step attenuator following the GR oscillator permitted adjustment of the rf field strength. The external applied magnetic field was also produced by a Helmholtz coil pair. The calculated inhomogeneity of the field over the effective cell volume was less than 0.1%. In practice the laboratory gradients due to surrounding ferrous equipment determined the gradients. The current to the Helmholtz coils could be varied to provide a slow scan of the magnetic field. The detector output was synchronously detected at 400 Hz, and the output recorded as a function of external magnetic with an X-Y recorder.

III. OPTICAL PUMPING OF NEON METASTABLE ATOMS

A. Method

Of the eight optical transitions that connect the metastable 3^3P_2 level to the $2p$ levels (Paschen notation), the 6402 Å line is the most intense and is strongly absorbed by the metastable neon atoms. Transitions induced by the circularly polarized 6402 Å resonance radiation will result in an accumulation of metastable atoms in states of greatest or least m_J, depending upon the sense of circular polarization. The degree of orientation produced by the optical-pumping cycle may readily be shown to be proportional to the intensity of the resonance radiation and the lifetime of the atom in a given m_J level. The optical magnetic-resonance signal amplitude depends in turn on the orientation produced and the intensity of the light beam which monitors the cell transparency.

Typical bright resonance lamps are characterized by pumping times on the order of 10^{-3} to 10^{-4} sec. The optical-pumping time is the relaxation time of the atom due to the resonance radiation. If the spin-state relaxation time is much shorter than the optical-pumping time, the orientation of the spin system will be severely limited, the magnetic-resonance linewidth will be very broad, and the detected signal very weak. Conversely, if the spin relaxation time is not small compared with the pumping time, an appreciable spin polarization can occur, and the magnetic-resonance signals can be easily observed.

Figure 2 is a recording of the change in the intensity of the transmitted light at 6402 Å (3^3P_2–3^3D_3) which occurs when the external magnetic field is slowly swept through the resonance condition. The lock-in time constant for this trace is 0.1 sec. The linewidth is slightly rf broadened, and has a width of approximately 30 kHz. Approximately 28% of the 6402 Å pumping light incident on the cell is absorbed by the $^3P_2$ metastable atoms, and the fractional change in the absorbed light at resonance is about 2×10^{-3}.

Figure 3 is obtained when the monochromator is scanned over the wavelength range 5700–

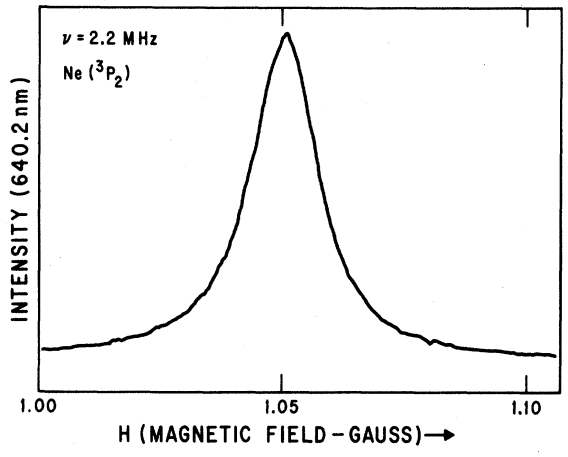

FIG. 2. Magnetic-resonance signal of $^3P_2$ neon atoms. The line is slightly rf broadened. Lock-in time constant is 0.1 sec.

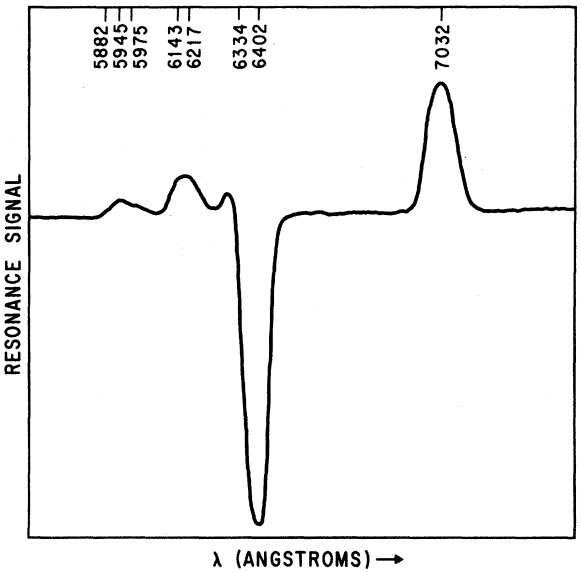

FIG. 3. Wavelength scan of transmitted light at the resonance condition. Resonances are observed at all eight transitions between $^3P_2$ and $2p^53p$ levels.

7200 Å. This range includes all the transitions between the $^3P_2$ metastable level and the levels of the $2p^53p$ configuration. The interesting feature here is that the resonance signal at 6402 Å has a phase opposite to all the other resonance signals. The reason for this is easily seen from the expression for the optical signal for the various levels. Thus, we find for the change in the transmitted light intensity as the sample becomes optically pumped

$$\Delta I(6402\ \text{Å}) \alpha 15(n_{+2} - \tfrac{1}{5}n) + 10(n_{+1} - \tfrac{1}{5}n) + 6(n_0 - \tfrac{1}{5}n) + 3(n_{-1} - \tfrac{1}{5}n) + (n_{-2} - \tfrac{1}{5}n) \ , \qquad (1)$$

and

$$\Delta I(7032\ \text{Å}) \alpha (n_0 - \tfrac{1}{5}n) + 3(n_{-1} - \tfrac{1}{5}n) + 6(n_{-2} - \tfrac{1}{5}n) \ , \qquad (2)$$

where n_m is the population of the magnetic sublevel whose magnetic quantum number is m, and n is the total population of the $^3P_2$ level. For a given distribution leading to a polarization, it is apparent that the optical signals for the two above cases will have opposite phase.

If the transmitted light is viewed directly without the benefit of a monochromator, the resulting resonance signal is an average over the individual signals for the various transitions shown in Fig. 3. This average is substantially smaller than the signal obtained at either 7032 or 6402 Å. In practice it was difficult to obtain a signal without the use of a monochromator. This results from a combination of the reduced signal strength and the large increase in the intensity of the nonresonant radiation reaching the detector.

B. Measurement of g_J Factor

Since both the resonance lamp and absorption cell contained helium and neon gas, it was possible to optically pump both the neon and helium metastable atoms and detect the magnetic resonance of each species separately. The polarization process was alternated between the two, merely by changing the polarizing elements and changing the interference filters in front of the detector. The resonance frequency at the absorption-line center in a constant external magnetic field was determined for both species. Since the optically pumped volumes were similar, the effects of field inhomogeneities on the frequency measurements was minimized. Rapid alternation (10 sec) between the helium and neon signals reduced the influence of drift in the external magnetic field. From the ratio of the resonance frequencies at constant field and the measured g factor for metastable helium,[14] we obtain $g_J(\text{Ne}: {}^3P_2) = 1.501\,52 \pm 0.000\,64$ in good agreement with the more precise atomic beam resonance measurements of Lurio *et al.*[15]

C. Polarization of Neon Atoms by Transfer Collisions with Helium

While making the g_J-factor measurements described in the preceding section, we observed that the metastable helium resonance at $g_J = 2$ altered the polarization of the neon atoms. In the absorption cell the helium metastable density is quenched in part by collisions with ground-state neon atoms in which

$$\text{He}(2^3S_1) + \text{Ne}(^1S_0) \rightarrow \text{He}(1^1S_0) + \text{Ne}(4^3P_2)$$
$$(\uparrow\uparrow) + (\uparrow\downarrow) \rightarrow (\uparrow\downarrow) + (\uparrow\uparrow)$$

followed by radiative decay to lower-lying levels. If a component of spin angular momentum is conserved in a collision in which this energy transfer to the neon occurs, the excited neon atoms will acquire a spin polarization which will manifest itself as an anisotropy of the polarization of the light emitted following radiative decay. We were able to observe a change in the intensity of the σ^+ polarized component of light emitted by the neon atoms parallel to the direction of the external magnetic field when the helium metastable atoms were optically pumped. In particular the $2s_5 - 2p_6$, $2p_9$, $2p_{10}$ transitions at 1.2066, 1.1177, and 0.9665 μ, respectively, showed a change in the relative intensity of the σ^+ radiated component as the helium metastable atoms were alternately spin polarized and depolarized. This indicates that neon atoms in the $2s_5$ level are spin polarized. The signal reversed phase when the σ_- component was monitored, and disappeared when the circular analyzer was removed. The fractional change in the emitted light is given by

$$f = [I(\sigma^+) - I(\sigma^-)] / [I(\sigma^+) + I(\sigma^-)] \ . \qquad (3)$$

Experimentally we obtain $f = 2 \times 10^{-3}$ which is comparable to the similar quantity for the forward scattered helium resonance radiation at 1.083 μ. Polarization changes are also observed in a number of cascade transitions from the $2p_{2,4,6,8,9,10}$ levels to the $1s_{2-5}$ levels, indicating that many of these levels are also spin polarized. We believe this is the first observation of spin exchange which accompanies significant energy transfer.[16]

Since the $2s_5$ level of neon can be polarized in this manner one can, in principle, obtain the magnetic-resonance signal of this state. The radiative decay time is on the order of 10^{-7} sec, so that rf magnetic fields on the order of a gauss are required. At low pressures the linewidth is determined by the radiative decay time, while at higher pressures collisional depolarization is more important. Alternatively, one could measure the quantity f defined in Eq. (3) as a function of the helium buffer pressure and obtain the same information.

IV. DEPOLARIZATION CROSS SECTION

The magnetic-resonance linewidth is determined by the relaxation time of the atom in a given Zeeman level, the lifetime of the $^3P_2$ metastable atom, the influence of the rf magnetic field, and inhomogeneities in the external magnetic field. The relaxation time of the neon metastable atoms in their Zeeman sublevels is determined by depolarizing collisions with ground-state neon ($^1S_0$) and ground-state helium ($^1S_0$) atoms both of which are magnetically inert. This collision-induced relaxation time can be written as

$$T_2 = (\sigma v N)^{-1} \ , \tag{4}$$

where σ is the effective geometric cross section, v is the mean relative velocity between collision partners, and N is the density of the helium or neon ground-state buffer atoms. In a cell containing both helium and neon gas, the relaxation time is given by

$$1/T_2 = 1/T_a + 1/T_b \ , \tag{5}$$

where T_a and T_b are given by Eq. (4) for helium and neon, respectively.

The relaxation time $T_{a(b)}$ can then be interpreted as the mean time between depolarizing collisions with helium (neon) ground-state atoms. In Lorentzian (lifetime-limiting relaxation processes) resonance linewidths are related to the relaxation time by

$$\Delta\nu = 1/\pi T_2 \ , \tag{6}$$

where $\Delta\nu$ is the full width in frequency units measured between the half maximum points of the absorption line. This yields

$$\Delta\nu = \{3.54\times10^{16}\frac{273}{\pi T}\left[\frac{8KT}{\pi}\left(\frac{1}{m_1}+\frac{1}{m_2}\right)\right]^{\frac{1}{2}}\sigma\}p \ , \tag{7}$$

where T is the temperature in degrees Kelvin, m_1 and m_2 are the atomic masses of the respective collision partners, K is Boltzmann's constant, and p is the partial pressure in millimeters of Hg of the collision partner.

The lifetime of the metastable neon atom also contributes to the linewidth as a result of diffusion to the cell walls and inelastic collisions with the hot electrons of the active discharge. If the cell is sufficiently large and the buffer-gas pressure sufficiently high, the metastable lifetime can be made large compared to the mean time between depolarizing collisions. This process then makes a negligible contribution to the resonance linewidth. The resonance magnetic field H_1 utilized to induce transitions between the magnetic sublevels of the neon metastable atoms broadens the linewidth. For rf field intensities which are not excessively large, this contribution can be expressed as

$$\Delta H^2 = \Delta H_0^2 + kH_1^2 \ , \tag{8}$$

where H_1 is the resonance rf magnetic intensity, ΔH is the observed linewidth, and ΔH_0 is the linewidth due to field gradients and relaxation processes. The influence of H_1 on the linewidth can be eliminated by measuring the linewidth as a function of H_1. A plot of (linewidth)^2 versus H_1^2 is then a linear function which can be extrapolated to zero H_1 and the linewidth ΔH_0 determined. A plot of this type is shown in Fig. 4 for two different cell pressures. Similar curves for approximately 30 different cell pressures were obtained, and all subsequent references to linewidth measurements are those for which $H_1 \to 0$.

The linewidth can now be represented by an equation of the form

$$\Delta\nu = Ap(\mathrm{Ne}) + Bp(\mathrm{He}) + C \ , \tag{9}$$

where $\Delta\nu$ is the measured linewidth as defined in Eq. (6), and A and B are constants defined by the bracketed portion of Eq. (7) for neon and helium, respectively. C is a constant which is determined by the field inhomogeneities across

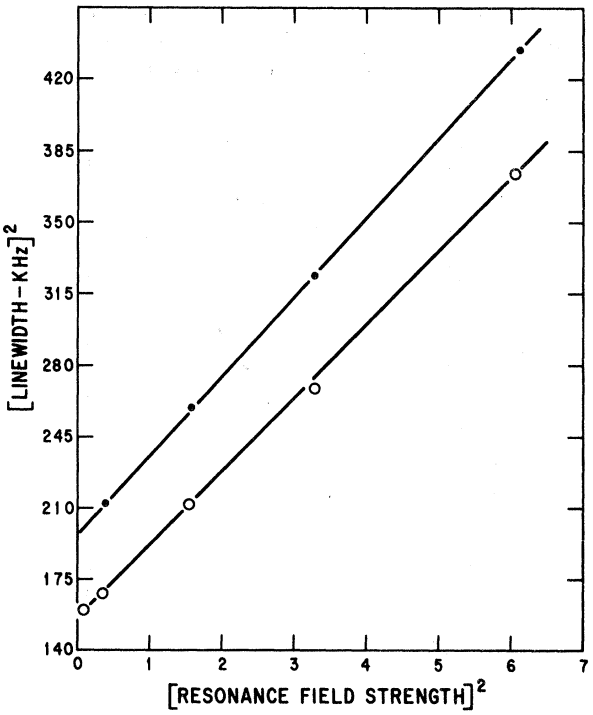

FIG. 4. Plot of square of measured linewidth versus square of rf field strength. The linewidth is extrapolated to zero H_1. The results obtained for two sample cells are shown. In the upper curve p(He) = 0.67 mm Hg and p(Ne) = 2.8 μHg, and for the lower curve p(He) = 0.6 mm Hg and p(Ne) = 2.2 μHg.

the sample cell and any other pressure independent contributions to the linewidth.[17]

For each of four absorption cells containing 2, 8, 24, and 40 μ Hg of neon, respectively, and a constant buffer of 0.2 mm Hg helium, the resonance linewidth was obtained in the limit of vanishing rf field. The results are shown in Fig. 5 as the open circles. This process was repeated for six closed cells each containing 3 μ Hg of neon and 0.16, 0.19, 0.46, 0.67, 0.78, and 1.15 mm Hg of helium, respectively. These data are shown as the open circles in Fig. 6.

A final series of resonance linewidth measurements were made with a cell which remained connected to the vacuum system and filled to a variety of relative pressures of helium and neon. All the data were fit to Eq. (9), and values for the constants A, B, and C obtained. The solid lines of Figs. 5 and 6 are plots of Eq. (9) with $A = 1.35 \pm 0.07$ MHz/mm Hg, $B = 60.8 \pm 3.0$ kHz/mm Hg, and $C = 9 \pm 0.5$ kHz for the condition described. In Fig. 5 the slope of the curve gives the rate of change of the linewidth due to changes in the neon partial pressures. The intercept gives the linewidth due to 0.2 mm Hg of helium plus field inhomogeneities across the sample volume. In Fig. 6 the slope gives the rate of change of linewidth with changes in helium pressure while the intercept is the residual linewidth due to gradients and 3 μ Hg of neon. The data points in Fig. 5 labelled with crosses were taken

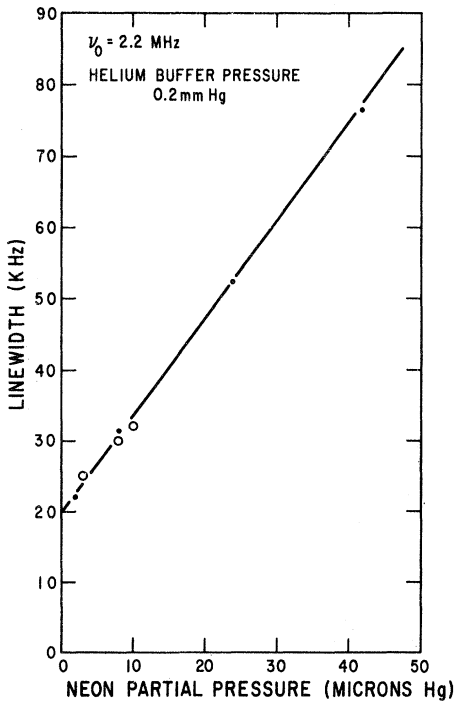

FIG. 5. Linewidth in frequency units versus the partial pressure of neon in μHg.

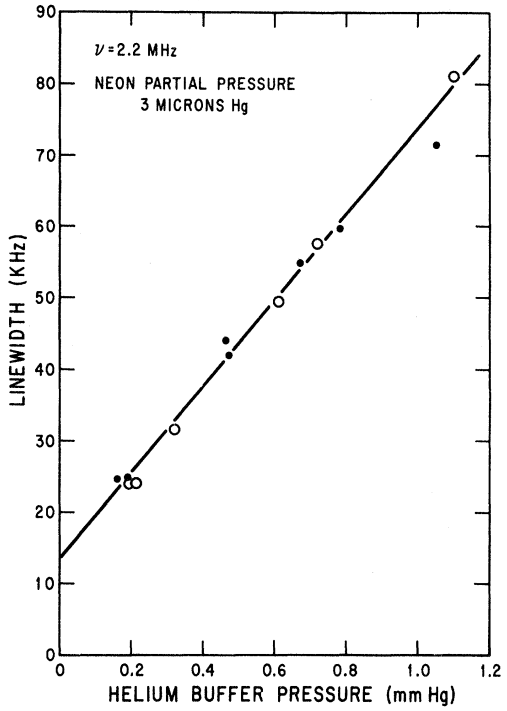

FIG. 6. Linewidth in frequency units versus the partial pressure of helium in mm Hg.

with the cell attached to the vacuum system. For these points the helium buffer pressure was 0.6 mm Hg, and 24.3 kHz was subtracted from each linewidth measurement in order to normalize it to the 0.2 mm Hg data. The crosses in Fig. 6 were obtained with 7 and 10 μ Hg of neon and various buffer pressures of helium after the linewidth was normalized to 3 μ Hg of neon.

The relaxation time due to depolarizing collisions is related to the linewidth by Eq. (6) and to the depolarization cross section by Eq. (7). From this we obtain the depolarization cross section for collisions between neon ($^3P_2$) and helium ($^1S_0$) atoms

$$\sigma(\mathrm{Ne}^M - \mathrm{He}) = 4.30 \pm 0.22 \times 10^{-17}\ \mathrm{cm}^2\ ,$$

and for collisions between metastable and ground-state neon atoms

$$\sigma(\mathrm{Ne}^M - \mathrm{Ne}) = 166 \pm 8 \times 10^{-17}\ \mathrm{cm}^2$$

at 300°K.

The gradient across the sample volume was determined to be 4.3 mG on the basis of the results obtained in Figs. 5 and 6. To provide an alternate check, the resonance linewidth of metastable helium was obtained at the same external magnetic field. The measured linewidth was 12.6 kHz in the limit of zero rf field. If the entire linewidth is ascribed to inhomogeneities, we find $\Delta H = 4.5$ mG in good agreement with the

value determined above.

These depolarization cross sections can be compared with their respective gas-kinetic cross sections determined from diffusion measurements: [18]

$$\sigma_D(\mathrm{Ne}^M - \mathrm{He}) = 40.5 \times 10^{-16}\ \mathrm{cm}^2\ ,$$

$$\sigma_D(\mathrm{Ne}^M - \mathrm{Ne}) = 42.7 \times 10^{-16}\ \mathrm{cm}^2\ .$$

This implies that approximately 100 collisions with ground-state helium atoms are required before a depolarizing collision occurs, while only three collisions with a neon ground-state atom is sufficient to cause a depolarizing transition.

The largest source of error occurs in the determination of the neon and helium pressures in the absorption cells. Accumulated errors in reading the McLeod gauge and cell tip-off are estimated to be 5%. Linewidth measurements were made from resonance signals in which the S/N was always greater than 10. Changes in the field gradient due to a change in the effective optically pumped volume was on the order of 10%. [19] This, however, represents less than a 4% error at the narrowest observed linewidths. The final uncertainty is estimated to be ±5% for the cross section measurements.

V. CONCLUSIONS

The relatively small depolarization cross section obtained for neon metastable atoms in a buffer of $^1S_0$ helium atoms suggests that the spherical symmetry of the outer electron of the neon $^3P_2$ atom is comparatively effective in shielding the core electrons from perturbations caused by collisions with helium, but considerably less effective for collisions with $^1S_0$ neon atoms. Evidently the increased polarizability of the neon atoms strongly influences the observed depolarization cross sections. In an effort to substantiate this, we have attempted to optically pump the $^3P_2$ atoms of argon and xenon in buffers of noble-gas ground-state atoms. We find in the case of $\mathrm{Ar}(^3P_2)$ that the depolarization cross section increases with the polarizability of the buffer gas, and approaches the diffusion cross section for collisions with ground-state argon atoms.

At low-gas pressures where atom-atom collisions are infrequent, the resonance linewidth is determined by the wall diffusion time. Under these conditions the magnetic-resonance signals of optically pumped $^3P_2$ atoms of the heavy noble gases are large and easily observed on the oscilloscope without narrow banding. The effects of collisions with buffer atoms is easily observed, and collisional depolarization cross sections can be obtained for a wide variety of metastable ground-state noble-gas mixtures. Both Xe and Kr have isotopes with nonzero nuclear spin. In this case spin-exchange collisions between the metastable and ground-state atom can result in a nuclear polarization and the ground-state magnetic resonances observed. The large available signals suggest that a wide variety of collisional effects, g factors, and hyperfine splittings can be studied for the heavy noble gases.

ACKNOWLEDGMENTS

I wish to thank especially F. A. Franz and H. B. Bebb for a number of stimulating discussions relating to the depolarization cross-section measurements. The help of F. D. Sinclair in all stages of this research is gratefully acknowledged.

---

[1] H. G. Dehmelt, Phys. Rev. 105, 1487 (1957).

[2] A. L. Bloom, J. Phys. Radium 19, 881 (1958).

[3] W. Franzen, Phys. Rev. 115, 850 (1959).

[4] B. Cagnac, J. Brossel, and A. Kastler, Compt. Rend. 246, 1827 (1958).

[5] F. D. Colegrove and P. A. Franken, Phys. Rev. 119, 680 (1960).

[6] L. D. Schearer, Advances in Quantum Electronics (Columbia University Press, New York, 1961), p. 239.

[7] The method of optical pumping has been recently extended to ions in their ground state. See, H. Ackermann, G. Zu Putlitz, and E. W. Weber, Phys. Letters 24A, 567 (1967).

[8] It has been suggested that states of $J = \frac{1}{2}$ ($L \neq 0$) would not be subject to such collisional relaxation as a result of selection rules on Δm_J. See, for example, F. A. Franz and J. A. Franz, Phys. Rev. 148, 82 (1966). This has been experimentally verified by Alan Gallagher, Phys. Rev. 157, 68 (1967), for the $^2P_{1/2}$ levels of Rb and Cs in buffers of He, Ar, and Ne. However, F. A. Franz, G. Leutert, and R. T. Shuey, Helv. Phys. Acta 40, 778 (1967), were unsuccessful in their attempt to optically pump the ($^2P_{1/2}$) ground state of thallium.

[9] The depolarization cross section for $^3P_2$ Hg atoms in collision with noble-gas atoms range from 0.71×10^{-14} cm^2 for He to 2.91×10^{-14} cm^2 for Xe. Klaus Tittel, Z. Physik 187, 421 (1965); B. Pitre, A. G. A. Rae, and L. Krause, Can. J. Phys. 44, 731 (1966).

[10] R. A. Bernheim, J. Chem. Phys. 36, 135 (1962).

[11] L. W. Anderson and A. T. Ramsey, Phys. Rev. 132, 712 (1963).

[12] Consequently, the polarizability of the noble-gas metastable atom is similar in magnitude to the polarizability of the adjacent alkali atom. Both possess large

polarizabilities due almost entirely to the spatial extent of the outer *s* electron. See, for example, E. J. Robinson, J. Levine, and B. Bederson, Phys. Rev. 146, 95 (1966).

[13]L. D. Schearer, Phys. Rev. Letters 21, 600 (1968).

[14]V. W. Hughes, G. Tucker, E. Rhoderick, and G. Weinreich, Phys. Rev. 91, 828 (1953).

[15]A. Lurio, G. Weinreich, C. W. Drake, V. W. Hughes, and J. A. White, Phys. Rev. 120, 153 (1960).

[16]Spin exchange collisions between metastable and ground-state helium have been observed as well as charge transfer between metastable Xe and the Xe ion. These are both cases of resonance energy transfer between similar atoms, however.

[17]We assume here that the contribution of the gradient adds linearly to the intrinsic linewidth due to collisions. This is usually true for small gradients. See, for example, A. Abragam, The Principles of Nuclear Magnetism (Clarendon Press, Oxford, England, 1961), pp. 50–51.

[18]J. R. Dixon and F. A. Grant, Phys. Rev. 107, 118 (1957).

[19]Included in this are linewidth changes associated with pumping light induced relaxation and with the discharge products. Linewidth changes of the neon resonance due to these effects were not observed. The estimate of 10% above as determined from measurements on optically pumped 2^3S_1 helium, where apparent linewidth changed approximately 1 kHz when going from a bright discharge at 0.2 Torr to a weak discharge at 1 Torr. This is presumably due to a change in the effective pumping volume.